Supplemental Information

Anode co-valorization for scalable and sustainable electrolysis

Joshua Jack[a,b], Wenjin Zhu[c], José L. Avalos[b,d], Jinlong Gong[c], Zhiyong Jason Ren [a,b]*

[a] Department of Civil and Environmental Engineering, Princeton University, Princeton, New Jersey 08544, USA

[b] The Andlinger Center for Energy and the Environment, Princeton University, Princeton, New Jersey 08544, USA

[c] Key Laboratory for Green Chemical Technology of Ministry of Education, School of Chemical Engineering and Technology, Tianjin University, Tianjin 300072, China.

[d] Department of Chemical and Biological Engineering, Princeton University, Princeton, New Jersey 08544, USA

S1.0 Standard redox potentials and operating voltages

In some cases the standard redox potentials of oxidations (E_{Rxn}^0) needed to be calculated using Eq. 1 (below)

$$Eq.\ 1)\ \ E_{Rxn}^0 = \frac{1}{nF}\sum (v_p)\Delta G_{fp}^0 - \sum (v_r)\Delta G_{fr}^0$$

Where v is the stoichiometric coefficient, ΔG_f^0 is the Gibbs free energy of formation of the product or reactant, n is the moles of electrons transferred, and F is

Faraday's constant (96,485 C/mol). The standard Gibbs free energies are available via various resources[1,2] or can be estimated using the Joback method[3].

To effectively compare operating voltages, all anode potentials from literature were converted to the reversible hydrogen electrode (E_{RHE}) scale using Eq. 2 (below)

$$Eq.2) \quad E_{RHE} = E_{SHE} + (0.059)(pH)$$

Where E_{SHE} is the potential of the standard hydrogen electrode under standard conditions (P =1 bar, T = 298.15K, pH = 0) and the pH of the anode electrolyte is used.

S2.0 Percent energy saving calculations

For the UOR we first compared the standard redox potential of 70mV for UOR vs. 1.23V for OER (94% greater). Later we compared the reported cell potential of 1.36V to the OER for HER assuming overpotentials of 0.37V and 0.05V (refs. in table S2), respectively, leading to an 18% decrease. In a similar manner, we compared the ethanol oxidation potential of 0.7V vs. OER at 1.23V and overpotentials of 0-0.37V (i.e. 56%).

S3.0 Energy inputs and costs calculations

We first calculate the charge required (Coulombs) to create 1kg of product by rearranging the Faradaic efficiency equation and assuming a modest efficiency value of 90%

$$Eq.3)\ Mass\ (kg)\ \times\ \left(\frac{1000g}{kg}\right) \times \frac{1}{M}\ n\ x\ F \times \frac{1}{FE/100}$$

where M is the molar mass, n is mole electron equivalents transferred per mol product, F is Faraday's constant (96485 C/mol e-), and FE is the Faradaic efficiency

Next we convert the total charge (C= A*seconds) to kWh/kg by converting seconds to hours and multiplying by the operating potential. For each oxidation scenario we use a practical operating potential based on literature values [Table S2]. We then calculate the direct energy costs of electrolysis by multiplying the kWh/kg by cost of electricity ($/kWh). A range of electricity costs from different sources were taken directly from the recent EIA Report for Levelized Cost and Levelized avoided costs of New Generation Resources in the Annual Energy Outlook 2020 [4]. Market value of the products were obtained from various sources listed in Table S2.

S4 Brief comparison to bioethanol energy costs

As described in section S3 (above), the estimated energy costs were calculated assuming a moderate FE of 90% and conservative estimates for overpotential

(Table S2). This led to the lowest energy cost estimates of around $522 per tonne ($1.56 per gallon) using AC_{Ox} via solar PV. Current bioethanol prices currently range from about $0.88 to $2.17 per gallon [5–7]. In addition, they can typically consume about 4.6-7.94 KwH/kg depending on processing conditions [converted from BTU/gallon, ref. [8]]. Interestingly, if overpotentials can be minimized and efficiencies can reach near unity, AC_{Ox} could theoretically produce ethanol at around 0.489 kWh/kg (about a tenth of bioethanol energy use) at much lower prices than bioethanol of around $0.04-0.065 per gallon via solar PV. Similarly, an optimized DI-OER process could generate ethanol at around 7.97 kWh/kg leading to a spot price of around $0.65-1.06 per gallon ethanol on solar PV.
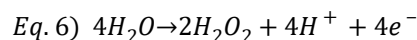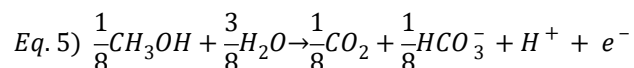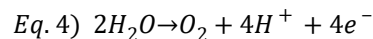
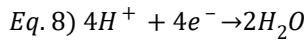**S5 Los Angeles, California case study calculations**

In this case study we assess the feasibility of satisfying 20% of LA's yearly energy demand with electrolysis. Based on the LA Department of Water and Power's reported annual energy demand[9], this amounts to a total of about 26 million MWh. For this scenario, we consider transforming this energy demand into H_2 and calculate the mass of H_2 (kg) required using an energy density of 33.6 kWh/kg[10]. We again assume a modest, FE of 90% and use Eq. 3 to calculate the amount of charge required for electrosynthesis. Next we convert the total charge (C= A*seconds) to kWh/kg by converting seconds to hours and multiplying by the operating potentials listed in Table S2. We then calculate the direct energy costs of electrolysis by multiplying the kWh/kg by cost of electricity

($/kWh). Energy costs projected from current CA rate in EIA, Electric Power Monthly[11].

Next we calculate the amount of direct water used for electrolysis per kg of H_2 production using 2.38 gallons/ kg H_2 (from mass balance). We assume a current cost of water of 6 ¢/gallon (based on LA's current non-residential water price, comparable to national average)[12]. We then include energy costs for in-plant water conveying and distillation of 0.0925 kWh/kg H_2O and 0.014 kWh/kg H_2O, respectively[13] . The total costs are then calculated by adding the direct energy costs, indirect energy costs, and direct water costs. For seawater and wastewater electrolysis, we assume no distillation energy is needed for anode reaction and in both cases electrolytes can be used as is. To calculate total profits, we calculate the total revenue assuming a H_2 selling price of $12.85 per kg[14].

Across the oxidation scenarios, we also calculate total yearly profits, assuming anode end-products can be sold. For the desired amount of H_2, we calculate the amount of anode products generated using a mass balance from the equations below:

$$Eq.\,4)\ \ 2H_2O{\rightarrow}O_2 + 4H^+ + 4e^-$$

$$Eq.\,5)\ \ \frac{1}{8}CH_3OH + \frac{3}{8}H_2O{\rightarrow}\frac{1}{8}CO_2 + \frac{1}{8}HCO_3^- + H^+ + e^-$$

$$Eq.\,6)\ \ 4H_2O{\rightarrow}2H_2O_2 + 4H^+ + 4e^-$$

$$Eq.\,7)\;\; HMF + H_2O \rightarrow FDCA + 6H^+ + 6e^-$$

$$Eq.\,8)\;\; 4H^+ + 4e^- \rightarrow 2H_2O$$
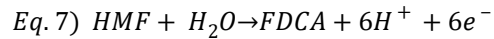
We then use various selling prices to calculate additional revenue. The total profits are then calculated by subtracting the total costs from the total revenues. For the 2040 estimates, we use the projected 2040 energy costs for solar photovoltaic (with credits) in EIA levelized energy report 2020[15]. In addition, we assume a sensible water increase per year is 7.3%, based on Covina, CA from the Department of energy water and wastewater annual price escalation rates for selected cities across the United States (2017)[16].

Supplemental Tables:

Table S1. Definition of acronyms used for oxidation reactions

Reaction shorthand	Reduced (electron donor)	Oxidized product
1,2P/LA	1,2-propanediol	Lactic acid
AC/CO2	Acetate	Carbon dioxide
BA or BZ /BZAL	Benzyl Alcohol	Benzaldehyde
Et or EtOH /Ac	Ethanol	Acetate
Gly/GCA	Glycerol	glyceraldehyde
Glu/GRA	Glucose	glucaric acid
HMF/FDCA	5-hydroxymethyl furfural	5-furandicarboxylic acid
Gly/GRA	Glycerol	glucaric acid
Cl/Cl2	chloride	chlorine
Cl/ClO	chloride	hypochlorite
SO3/SO4	Sulfur trioxide	Sulfate
Urea/CO2	Urea	Carbon dioxide

EG/GCA	Ethylene glycol	Glycolic acid

Table S2. Metrics used to assess oxidation reactions

Anodic rxn	Applied cell voltage Et (V)	Applied cell voltage H_2 (V)	Market value ($/kg)	Comments and voltage ref.
High-grade water OER	2.46	1.65	.024[17]	Table 1, [18]
Seawater OER	2.34	1.73	.024[17]	Fig. 4c, [19]
Microbial organic oxidation (for MEC)	2.4	0.83	.042[20]	[21]
Hydrogen peroxide generation	3.36	2.25	0.59[22]	[19,23,24]
HMF/FDCA oxidation	2.46	1.47	32[25]	[26]

Table S3: Metrics used to assess reduction reactions

Cathodic rxn	Overpotential (V)	Market value ($/kg)	Comments and voltage ref.
H_2 evolution	0.05	12.85[14]	[27]
CO_2 reduction to ethanol	0.95	(Not used)	[28]

Table S4: Products generated and water demands

Anode/Cathode reaction	Product amount (MT)	Process water demands (MGal)
Hydrogen	0.154	NA
High-grade water OER	2.4	370
Seawater OER	2.4	NA
Microbial organic oxidation (for MEC)	1.7	NA
Hydrogen peroxide generation	2.6	370

HMF/FDCA oxidation	8.05	370

Table S5: Comparison of select anode catalysts towards water electrolysis

Anode Reaction	Catalyst	Electrolyte	J_{obs} (mA/cm^2)	Scale (cm^2)[A]	Approx. material cost ($/kg)[B]	Stability (hours)[C]	Ref.
Glucose	NiFeOx	100mM glucose + 1M KOH	200	NA	0.2-19	24	[29]
Benzyl alcohol	hp-Ni	1M KOH +10mM BA	100	0.25	17-19	18	[30]
1,2-propanediol	Rh/C	2M KOH + 2M PD	367	0.2	8500-23300	48	[32]
Ethanol	Rh/C	2M KOH + Ethanol	492	0.2	8500-23300	48	[32]
HMF	Ni$_3$S$_2$	1M KOH + 10mM HMF	100	0.25	17-19	18	[33]
Ammonia	NiZnCu	1M KOH + 0.3M NH$_4$Cl	100	0.5	2-19	40	[34]
NaCl/Cl$_2$	RTO-DSA	5M NACl or 200 g/m3, pH 2-4	425	NA	970-11660	4380-8760	[35]
NaCl/ClO$^-$	RTO-DSA	5M NACl; 1-5 g/m^3 NaClO	275	NA	970-11660	4380-8760	[36]
Urea	Ni$_3$N	1M KOH+ 0.5M urea	100	.08[D]	17-19	36	[37]

[A] Based on reported working electrode; [B] Calculated per kg of active catalyst, range based on high and low values for each material used, cals. detailed below [C] Longest reported stable operation[D] mass active catalyst per cm^2

Table S6: Comparison of select anode catalyst towards CO_2 electrolysis

Anode Reaction	Catalyst	Electrolyte	J_{obs} (mA/cm^2)	Scale (cm^2)[A]	Estimated material cost ($/kg)[B]	Stability (hours)[C]	Ref.
Glycerol	Pt/C	2M KOH+ 2M Glycerol	96	1	2300-29100	2	[39]
Ethanol	Pd	4M KOH + 10% EtOH	12.5	6	25810-78000	6	[40]
HMF	NiO	0.5M $KHCO_3$ + 10mM HMF	2	0.5	17-19	3	[41]
1,2-propanediol	ACT-TEMPO/C	20mM 1,2 PD+ 0.5 M $KHCO_3$/ K_2CO_3	15	10	6480-22500	2	[42]
Glucose	Pt/C	2M KOH+ 2M Glucose	13	1	2300-29100	NA	[39]
$NaCl/Cl_2$	RuO_2-IrO_2-TiO_2 DSA	Sat. KCl solution (pH 2)	100	4	970-11660	8	[43]
$NaCl/ClO^-$	RuO2	0.5M NACl, pH 7.2	4.5	2	8520-23300	24	[44]
Urea	Ni foam	5 M KOH + 0.33 M urea	100	NA	590-660 per m^2	4	[45]
$SO_3{-}/SO_4{-}$	IrO_2 – Ta_2O_5	0.3M Na_2SO_3	10	25	120-150	5	[46]
Ammonia	Pt/C	5 M KOH + 1 M ammonia	10	0.5	2300-29100	4	[45]

[A] Based on reported working electrode; [B] Calculated per kg of active catalyst, range based on high and low values for each material used, cals. detailed below [C] Longest reported stable operation

Table S7: Approximate electrode material costs

Material	Price (USD/kg)	Ref.
Copper	9.33	[47]
Nickel	19.07	[47]
Aluminum	2.65	[47]
Zinc	2.95	[47]
Lead	2.45	[47]
Cobalt	51.17	[47]
Aluminum alloy	2.27	[47]
Tin	32.91	[47]
Iron	0.21	[47]
Titanium	4.80	[47]
Molybenum	26.00	[47]
Tantalum	151.80	[47]
Tantalum (2017)	128.00	[47]
Nickel (2014)	16.89	[47]
TEMPO	6480-22500	[48]
RTO-DSA[1]	966.00	[49]
Carbon cloth[1]	100-380 per m^2	[50]
Nickel foam[1]	590-660 per m^2	[51]
Gold	57564.54	[52]
Silver	766.47	[52]
Platinum	32111.80	[52]
Iridium	167183.64	[52]
Rhodium	549776.97	[52]
Palladium	78094.05	[52]
Ruthenium	23309.26	[53]
Ru (2019)	8519.94	[52]
Pd (2014)	25817.01	[52]

[1] Calculate based on surface area price from vendor [2] Past years used to provide range with pure metals

References.

1. UCDSB. Organic Compounds: Physical and Thermochemical Data. (2021). Available at: http://www2.ucdsb.on.ca/tiss/stretton/database/organic_thermo.htm.
2. Toolbox, E. Standard state and enthalpy of formation, Gibbs free energy of formation, entropy and heat capacity. (2021).
3. Joback, K. G. & Reid, R. C. Estimation of Pure-Component Properties from Group-Contributions. *Chem. Eng. Commun.* (1987). doi:10.1080/00986448708960487
4. Administration, U. . E. I. *Annual Energy Outlook 2020.* (2020).
5. Bušić, A. *et al.* Bioethanol production from renewable raw materials and its separation and purification: A review. *Food Technology and Biotechnology* (2018). doi:10.17113/ftb.56.03.18.5546
6. Rosales-Calderon, O. & Arantes, V. A review on commercial-scale high-value products that can be produced alongside cellulosic ethanol. *Biotechnology for Biofuels* (2019). doi:10.1186/s13068-019-1529-1
7. Mcaloon, A., Taylor, F., Yee, W., Ibsen, K. & Wooley, R. Determining the Cost of Producing Ethanol from Corn Starch and Lignocellulosic Feedstocks Determining the Cost of Producing Ethanol from Corn Starch and Lignocellulosic. *Agriculture* (2000). doi:NREL/TP-580-28893
8. Lorenz, D., Lorenz, D., Morris, D. & Morris, D. How Much Energy Does It Take to Make a Gallon of Ethanol? *Production* (2007).
9. LA Department of Water and Power. Power and Water Use: Past & Present. (2020). Available at: https://www.ladwp.com/ladwp/faces/ladwp/aboutus/a-water/a-w-pastandpresent?_adf.ctrl-state=6ousz4h30_4&_afrLoop=316877080154674. (Accessed: 10th July 2020)
10. Molloy, P. Run on Less with Hydrogen Fuel Cells - Rocky Mountain Institute. (2019). Available at: https://rmi.org/run-on-less-with-hydrogen-fuel-cells/. (Accessed: 13th July 2020)
11. Adminstration, E. I. Electric Power Monthly: February 2020. (2020).
12. Company, C. water service. Los Angeles County Region Non-residential metered service.
13. Webber, M. E. The water intensity of the transitional hydrogen economy. *Environ. Res. Lett.* 034007 (2007).
14. Partnership, C. F. C. Cost to refill. (2020). Available at: https://cafcp.org/content/cost-refill. (Accessed: 13th July 2020)
15. Adminstration, U. S. E. I. *Levelized Cost and Levelized Avoided Cost of New Generation Resources in the Annual Energy Outlook 2020.* (2020).
16. U.S DOE. *Water and Wastewater Annual Price Escalation Rates for Selected Cities across the United States.* (2017).
17. Dorris, C. C., Lu, E., Park, S. & Toro, F. H. High-Purity Oxygen Production Using Mixed Ionic-Electronic Conducting Sorbents. *Sr. Des. Reports*

(2016).

18. De Luna, P. *et al.* What would it take for renewably powered electrosynthesis to displace petrochemical processes? *Science* **364**, (2019).

19. Tong, W. *et al.* Electrolysis of low-grade and saline surface water. *Nature Energy* **5**, 367–377 (2020).

20. Pilorgé, H. *et al.* Cost Analysis of Carbon Capture and Sequestration of Process Emissions from the U.S. Industrial Sector. *Environ. Sci. Technol.* (2020). doi:10.1021/acs.est.9b07930

21. Lu, L. *et al.* Wastewater treatment for carbon capture and utilization. *Nature Sustainability* **1**, 750–758 (2018).

22. Database, I.-I. C. P. Hydrogen Peroxide Prices: Historical & Current. (2020). Available at: https://www.intratec.us/chemical-markets/hydrogen-peroxide-price. (Accessed: 10th July 2020)

23. Garlyyev, B., Xue, S., Fichtner, J., Bandarenka, A. S. & Andronescu, C. Prospects of Value-Added Chemicals and Hydrogen via Electrolysis. *ChemSusChem* (2020). doi:10.1002/cssc.202000339

24. Shi, X. *et al.* Understanding activity trends in electrochemical water oxidation to form hydrogen peroxide. *Nat. Commun.* (2017). doi:10.1038/s41467-017-00585-6

25. Zauba. Detailed Export Data of 2 5 furandicarboxylic acidle. (2021).

26. Liu, W. J. *et al.* Electrochemical oxidation of 5-hydroxymethylfurfural with NiFe layered double hydroxide (LDH) nanosheet catalysts. *ACS Catal.* (2018). doi:10.1021/acscatal.8b01017

27. Neyerlin, K. C., Gu, W., Jorne, J. & Gasteiger, H. A. Study of the Exchange Current Density for the Hydrogen Oxidation and Evolution Reactions. *J. Electrochem. Soc.* (2007). doi:10.1149/1.2733987

28. Li, F. *et al.* Cooperative CO2-to-ethanol conversion via enriched intermediates at molecule–metal catalyst interfaces. *Nat. Catal.* (2020). doi:10.1038/s41929-019-0383-7

29. Liu, W. J. *et al.* Efficient electrochemical production of glucaric acid and H2 via glucose electrolysis. *Nat. Commun.* (2020). doi:10.1038/s41467-019-14157-3

30. You, B., Liu, X., Liu, X. & Sun, Y. Efficient H2 Evolution Coupled with Oxidative Refining of Alcohols via A Hierarchically Porous Nickel Bifunctional Electrocatalyst. *ACS Catal.* (2017). doi:10.1021/acscatal.7b00876

31. Wang, D. *et al.* Direct electrochemical oxidation of alcohols with hydrogen evolution in continuous-flow reactor. *Nat. Commun.* **10**, 1–8 (2019).

32. Pagliaro, M. V. *et al.* Carbon supported Rh nanoparticles for the production of hydrogen and chemicals by the electroreforming of biomass-derived alcohols. *RSC Adv.* (2017). doi:10.1039/c7ra00044h

33. You, B., Liu, X., Jiang, N. & Sun, Y. A General Strategy for Decoupled Hydrogen Production from Water Splitting by Integrating Oxidative Biomass Valorization. *J. Am. Chem. Soc.* (2016). doi:10.1021/jacs.6b07127

34. Hu, S. *et al.* Synthesis of N doped NiZnCu-layered double hydroxides with reduced graphene oxide on nickel foam as versatile electrocatalysts for hydrogen production in hybrid-water electrolysis. *J. Power Sources* (2020). doi:10.1016/j.jpowsour.2020.227872

35. Franco, F., Prior, J., Velizarov, S. & Mendes, A. A systematic performance history analysis of a chlor-alkali membrane electrolyser under industrial operating conditions. *Appl. Sci.* (2019). doi:10.3390/app9020284

36. Karlsson, R. K. B. & Cornell, A. Selectivity between Oxygen and Chlorine Evolution in the Chlor-Alkali and Chlorate Processes. *Chemical Reviews* (2016). doi:10.1021/acs.chemrev.5b00389

37. Hu, S. *et al.* Ni 3 N/NF as Bifunctional Catalysts for Both Hydrogen Generation and Urea Decomposition. *ACS Appl. Mater. Interfaces* (2019). doi:10.1021/acsami.8b19052

38. Zhang, J. Y. *et al.* Energy-saving hydrogen production coupling urea oxidation over a bifunctional nickel-molybdenum nanotube array. *Nano Energy* (2019). doi:10.1016/j.nanoen.2019.04.035

39. Verma, S., Lu, S. & Kenis, P. J. A. Co-electrolysis of CO2 and glycerol as a pathway to carbon chemicals with improved technoeconomics due to low electricity consumption. *Nat. Energy* (2019). doi:10.1038/s41560-019-0374-6

40. Bevilacqua, M. *et al.* Energy Savings in the Conversion of CO2 to Fuels using an Electrolytic Device. *Energy Technol.* (2014). doi:10.1002/ente.201402014

41. Choi, S. *et al.* Mechanistic Investigation of Biomass Oxidation Using Nickel Oxide Nanoparticles in a CO2-Saturated Electrolyte for Paired Electrolysis. *J. Phys. Chem. Lett.* (2020). doi:10.1021/acs.jpclett.0c00425

42. Pérez-Gallent, E. *et al.* Electroreduction of CO2 to CO Paired with 1,2-Propanediol Oxidation to Lactic Acid. Toward an Economically Feasible System. *Ind. Eng. Chem. Res.* (2019). doi:10.1021/acs.iecr.8b06340

43. Guo, J. H. & Sun, W. Y. Integrating Nickel-Nitrogen Doped Carbon Catalyzed CO2 Electroreduction with Chlor-Alkali Process for CO, Cl2 and KHCO3 Production with Enhanced Techno-Economics. *Appl. Catal. B Environ.* (2020). doi:10.1016/j.apcatb.2020.119154

44. Quan, F. *et al.* Highly efficient electrochemical conversion of CO2 and NaCl to CO and NaClO. *Green Chem.* (2019). doi:10.1039/c9gc01099h

45. Medvedeva, X. V., Medvedev, J. J., Tatarchuk, S. W., Choueiri, R. M. & Klinkova, A. Sustainable at both ends: electrochemical CO2utilization paired with electrochemical treatment of nitrogenous waste. *Green Chem.* (2020). doi:10.1039/d0gc01754j

46. Kong, Y. *et al.* Design of counter oxidation vs. CO2 electroreduction for efficient formate production on a tin cathode. *J. Electroanal. Chem.* (2019). doi:10.1016/j.jelechem.2019.113264

47. Metalary. (2021). Available at: https://www.metalary.com/.

48. Sigma Aldrich.

49. ElectrodeSupply.

50. FuelCellStore.

51. Mtixtl.
52. Mining.com. Available at: https://www.mining.com/markets/.
53. Statistica-Rh